### Made available by Hasselt University Library in https://documentserver.uhasselt.be

Liquid Identification in a Microplate Format Based on Thermal and Electrical Sensor Data Fusion

Peer-reviewed author version

GOOSSENS, Juul; BORMANS, Seppe; OUDEBROUCKX, Gilles; VANDENRYT, Thijs; El Habti, Souhaib; MAHDAVINASAB, Seyedmohammad & THOELEN, Ronald (2022) Liquid Identification in a Microplate Format Based on Thermal and Electrical Sensor Data Fusion. In: IEEE sensors journal, 22 (20), p. 19809 -19817.

DOI: 10.1109/JSEN.2022.3202691

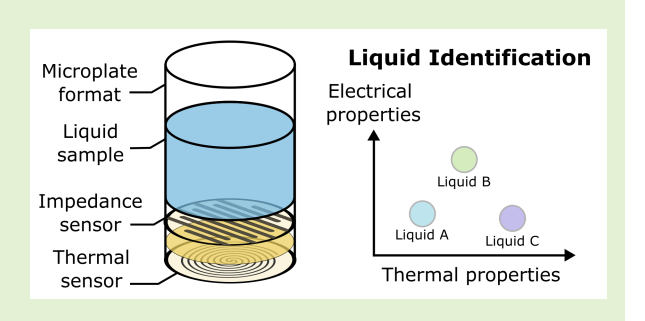
Handle: http://hdl.handle.net/1942/38842



# Liquid Identification in a Microplate Format based on Thermal and Electrical Sensor Data Fusion

Juul Goossens, Seppe Bormans, Gilles Oudebrouckx, Thijs Vandenryt, Souhaib El Habti, Mohammad Mahdavinasab, and Ronald Thoelen

Abstract—Multi-device synchronous measurement and thus a fusion of data from multiple sensor sources is becoming a fundamental but non-trivial task. Essentially, different sensors have their own limitations and uncertainties; the fusion of the data serves to increase the accuracy of performance. This research aims to expand the possibilities of multi-parameter sensing by integrating impedance and thermal sensors into a microplate format for the simultaneous assessment of electrical and thermal properties. The sensor uses a modified transient plane source measuring principle to monitor thermal changes and interdigitated electrodes for impedance analysis. The sensor is put to the test in the characterization of different glycerol and NaCl dilutions based on the varying thermal and electrical properties. At last,



to demonstrate the added value of data fusion for liquid identification, a proof-of-application experiment shows the identification of fruit juices based on both measurands using a Gaussian Mixture Model. These experiments already highlight the power of this combined measuring technology in simple liquid identification processes, hence showing great potential to develop advanced diagnostics in various fields such as healthcare, biology, or food quality by providing the ability to effectively perform parallel impedance and thermal based measurements.

Index Terms—Electrochemical Impedance Spectroscopy, Liquid Identification, Microplate Format, Thermal Sensing, Sensor Fusion

#### I. INTRODUCTION

SENSOR data fusion and integration refers to the technology to combine data from multiple sensors to achieve inferences that are not feasible from each sensor individually. Multi-device synchronous measurement and thus fusion of data from multiple sensor sources is becoming a fundamental aspect in research. Essentially, different sensors have their own limitation and uncertainties; the fusion of the data serves to increase the accuracy of performance. Briefly, the fusion of data can result in more enhanced and complementary perceptions and circumvent the drawbacks of each measuring

Manuscript received xx; revised xx; accepted xx. Date of publication xx; date of current version xx. This work was supported and funded by AgrEUfood and Food Screening, which is carried out with a contribution from the European programme Interreg Flanders-Netherlands and Euregio Maas-Rhine. (Juul Goossens and Seppe Bormans are co-first authors.)(Corresponding author: Juul Goossens)

The authors are with the Institute for Materials Research (IMO), Hasselt University, 3590 Diepenbeek, Belgium, and also with IMEC vzw, Division IMOMEC, 3590 Diepenbeek, Belgium (e-mail: juul.goossens@uhasselt.be; seppe.bormans@uhasselt.be; gilles.oudebrouckx@uhasselt.be; thijs.vandenryt@uhasselt.be; elhabti1999@outlook.com; mohammad.mahdavinasab@uhasselt.be; ronald.thoelen@uhasselt.be).

This article has supplementary material available at xx, provided by the authors.

technique itself. Additionally, as one key advantage of parallel processing, more timely information can be gathered when analysing a process in real-time [1], [2].

During the last few decades, a tremendous amount of research towards the development of diagnostic tools based on various sensing technologies has been conducted. There has been a huge interest because of the high versatility and broad application potential of these platforms. Different measuring principles can be drawn upon when establishing a measuring device. The choice of sensing principle will mainly be based on the property of interest. The most common sensing types are: electrochemical, optical, thermal, and mass-based [3], [4]. Within this research, two read-out techniques are combined to develop a multi-parameter sensing technology to monitor aqueous solutions. The device comprises two individually sensing elements on top of each other, *i.e.* thermal properties and electrical impedance sensing structures, incorporated into the bottom of a microplate.

The measurement of thermal properties can be deployed as sensing technology. The assessment of thermal properties in liquids can be done via hot wire techniques [5],  $2\omega$  or  $3\omega$  [6], or the Transient Plane Source (TPS) method [7]. The latter method, as introduced by Gustafsson et al. in 1979, has become an ISO standard (ISO 22007-2) to determine

thermal conductivity and thermal diffusivity of materials [8]. To determine the thermal properties of a given sample, all these above-mentioned methods rely on metal wire or film to produce heat when in contact to the sample. The effect of the heat on the sample can be characterized by the sensor's response. On this basis, the sensor design is rather simple since heating and temperature sensing is done with one single element. However, the TPS-method is a more straight-forward measuring principle as it is based on a DC current rather than AC. Additionally, it has already been proven effective in a microplate format [9]. Even though, up to now, the research on the TPS method has focused more on determining the thermal properties whereby the sample is static during measurement: solids [10], [11], liquids [12], [13], thin films [14], [15]. Furthermore, as already shown in our previous work, a modified version, adapted from the TPS method, was developed as a thermal read-out technique to monitor mixing ratio of liquids [16], the concentration of cell suspensions [17], and monitoring cell proliferation [9], [17].

Next, Electrical Impedance Spectroscopy (EIS) is a technique that has been widely used in a broad range of applications such as food screening [18], monitoring of corrosion [19], [20], characterization of solid electrolytes [21], and bioanalytical applications [18], [22]. In fact, almost any process which changes the conductivity of a system can be recognised by EIS, hence a multitude of properties can be elucidated using the technique [22]. EIS can essentially provide an electrical fingerprint of the sample and give insights into its properties and behaviour. Nonetheless, biological applications cover the majority of EIS research today [18], [23]–[25].

Sensor fusion only recently arose to bring novel and innovative insight into the general sensor research field. It can be seen in literature on electrical impedance-based sensing that by using the measurement values obtained at different frequencies or the extracted parameter of fitting impedance data already gives a significant advantage in many applications [26], [27]. Despite the great value of thermal property and electrical impedance analysis on their own, much less is known about the combination of both. Jaegle et al. [28] combined the analysis of thermal and electrical properties and showed the development of a small electronic tongue composed of a polyimide substrate containing different sensing elements for employing EIS and the  $3\omega$  method. This research already showed the potential of combined thermal and electrical impedance read-out for fluid characterization. The combined measuring platform has great potential to develop advanced diagnostics in various fields such as healthcare, biology, or food quality by providing the ability to effectively perform parallel impedance- and thermal based measurements, especially when successfully integrated in a high-throughput format. This research aims to expand the possibilities of multi-parameter sensing by integrating impedance and thermal sensors into a microplate format for the simultaneous assessment of electrical and thermal properties. Despite being both attractive read-out methods on their own, yet when successfully combined, could excel further and circumvent the most prominent disadvantages of each technique. For instance, in EIS, the measurements are highly influential to temperature fluctuations [29]. Furthermore, changes in the ion concentration of the medium can occur. Note that this sometimes can be desirable, depending on the application [30], [31]. Likewise, during thermal measurements on inhomogeneous samples, the measurements depend on the penetration depth and the thermal path between the subject under test and the sensor, which in some cases can be of interest [32].

#### II. MEASURING CONCEPT

As the thermal sensing concept is based on our earlier published work, the underlying mechanisms and principles of this in-house designed sensor are not explained in length, hence only the basics are clarified [9], [14], [17].

A TPS sensor consists of a metal heating structure which acts as a heat source as well as a temperature detector. Heat pulses are generated by sourcing a square wave current pulse through the meander (Joule heating). As a result of heating, the electrical resistance of the sensor elevates. In turn, the electrical resistance combined with the temperature coefficient of resistance ( $\alpha$ ) can be used to accurately determine the

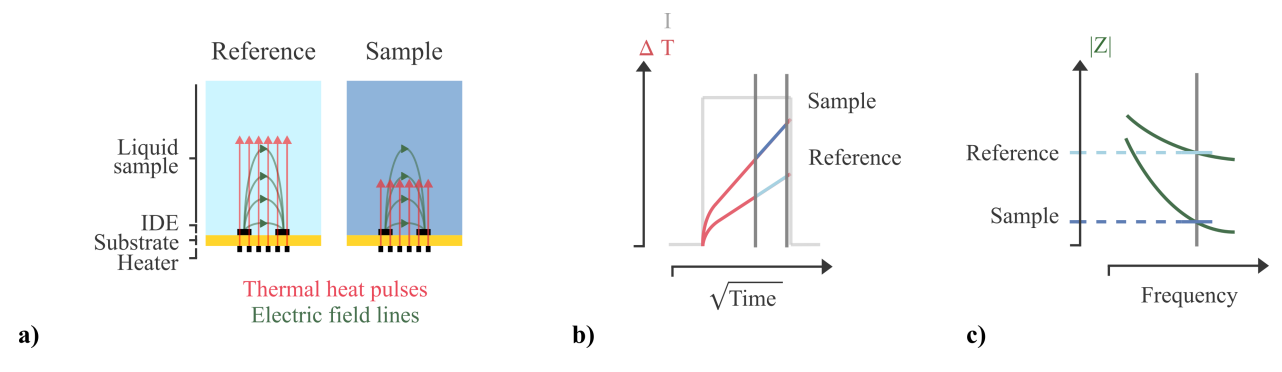


Fig. 1. **Measuring concept: a)** Schematic cross-section of a measuring sensor consisting of a thermal heater and an IDE structure. The heat pulses originating from the heater, and the propagating field lines from the IDE, are visualised using red and green arrows. The dissipation of heat, as well the electrical field, varies when examining liquids with different properties ( $e_{(REF)} > e_{(SAMPLE)}$ ),  $e_{(SAMPLE)}$ ), **b)** Conceptual thermal read-out method. Due to a lower heat dissipation by the sample, the temperature response of the sensor increases more steeply. In other words, the slope of the sensor's temperature gradient can give insight into the thermal effusivity. At this given slope interval, Slope (SAMPLE) is greater than Slope (REF). **c)** Conceptual electrical impedance read-out method. The impedance can be determined by measuring the resistance at different frequencies. In our case, the complex resistance will be determined at one specific frequency. A difference in impedance magnitude |Z| can be read out between the sample and reference (|Z| (REF) > |Z| (SAMPLE)).

sensor's temperature. Consequently, by looking at the temperature profile of the supplied pulse, the ability of the sensor to dissipate its produced heat to the sample can be determined [7], [10]. This way, the thermal effusivity (*e*) of the sample in contact, *i.e.* the ability to exchange heat with its surroundings, can be estimated.

Figure 1b conceptually describes the measurement of two samples with varying thermal effusivity. The temperature gradient of the sensor as a response to a block wave current pulse indicates the heat absorption capability of the sample. The slope of this transient curve over the square root of time reflects the thermal effusivity [10].

In contrast to this thermal sensing technique, EIS is already a well-established measuring technique in many fields for various applications. A frequency-dependent AC voltage is supplied to the sample. The corresponding current can be measured and used to calculate the magnitude of resistance |Z|. The influence of the frequency enables to study both the electrical resistive and capacitive properties. This can give insight into how the electrical properties change at the interface (double layer capacitance) of the electrodes within the lower frequency regime and in the bulk liquid (solution resistance) occurring at the higher frequency regime [33].

Figure 1c conceptually describes the measurement of two samples with varying electrical conductivity ( $\kappa$ ). The propagating electrical field, caused by the AC potential at the interdigitated electrode (IDE) structure, penetrates into the sample. The measured magnitude of resistance |Z| at various frequencies reflects the impedance of the liquid/sensor interface or the fluid resistance. With liquid identification in mind, this study focuses on the solution resistance at a higher measuring frequency [33].

#### III. MATERIALS AND METHODS

#### A. Sensor Setup

The presented sensor setup builds upon an earlier sensor design within our research group [9]. This earlier design integrated thermal sensors into a well plate format, which we combine together with integrated impedance sensing structures. The presented sensor setup is constructed by two main parts: a baseplate and a microplate. The microplate is equipped with integrated sensors and can entirely be attached onto the baseplate (Figure 2b).

A sensor strip is designed to fit underneath an 8-well plate, containing eight individual thermal and impedance sensing structures (Figure 2a). The thermal sensing element is located on the bottom side of a 25 µm thick polyimide substrate and therefore not making contact to the sample (electrically insulated). While on the other hand, the impedance sensor is located on the top side, situating itself in the wells, thus making direct contact to the sample. The thermal sensing element is a heater composed of a double spiral copper track ( $\varnothing = 5$  mm) with a height, width, and spacing between the tracks of respectively 12 µm, 60 µm, and 80 µm ( $R_{init} = 3.7 - 4.2 \Omega$ ,  $\alpha = 3.701 \times 10^{-3} \pm 0.031 \times 10^{-3} K^{-1}$ ). As the sensitivity is influences by the  $R_{init}$ , thin tracks were used to increase this parameter. The impedance sensor is composed of interdigitated

electrodes with spacing between the tracks of 300 µm and a width of the track of 300 µm (Figure 2a). With liquid identification in mind, the IDE tracks are much wider to achieve a deeper penetration depth into the bulk liquid. The impedance sensing element is finished with an electroplated gold layer to prevent sensor degradation while in contact to the sample. The sensor strips were produced externally (XPCB, China) using standard flexible Printed Circuit Board (PCB) manufacturing technology.

The microplate was CNC milled out of Acetal Copolymer (YouniQ Machining, Belgium) of which the dimensions are conform to 96-well plate standards [34], [35]. The material choice was mainly determined by its chemical resistance towards various solvent, which allows a broad range of fluids to be measured. Alignment holes are provided in the sensor strip for placement of the sensing elements perfectly in the middle of the wells ( $\emptyset = 7$  mm). The sensor strip attaches to the bottomless well plate via the adhesive side (467MP, 3M, United States). The adhesive has proven to be effective for a watertight seal (Figure 2a).

The microplate with integrated sensors can entirely be attached onto the PCB, which also functions as the base. This rigid PCB contains the wiring to form a connection between the sensor and the connected read-out equipment (Figure 2b). Spring-loaded (Pogo) pins integrated in the PCB forms the elegant connection to the contact pads on the sensor strips. The thermal (4-wire) and impedance (2-wire) readout equipment can be connected via the pin headers. For a more detailed description of the sensor wiring, please refer to the Supplementary Material. The PCB itself is surrounded in Polymethyl methacrylate (PMMA) spacers which provide cut-outs to make these above mentioned connections. One additional spacer-plate underneath the PCB provides trapped air pockets underneath the sensing elements (Figure 2b). The superior insulating property of air results in an approximately unidirectional transfer of heat from the heater towards the sample.

#### B. Instruments

Figure 3 shows the experimental setup and instruments used to perform the measurements. A desktop computer is used to control the measuring equipment and collect the data. For the thermal readout, custom LabVIEW software is used to control a source measure unit (PXIe-4139, NI, United States) coupled with a multiplexer (PXIe-2503, NI, United States). Additionally, commercially available software (PSTrace 5.7, PalmSens, The Netherlands) is used to control an impedance analyser (PalmSens 4, PalmSens, The Netherlands) in combination with a multiplexer (MUX8-R2, PalmSens, The Netherlands). It should be apparent that regardless of the geometry of the sensing structures, the read-out equipment could be used in a similar fashion. In that sense, the measuring setup works independently of the sensor characteristics. A real-life photograph of the measurement setup with connected hardware can be seen in the Supplementary Material.

The following thermal measuring settings were used to generate the heat pulses: heating time 1 s, heating power

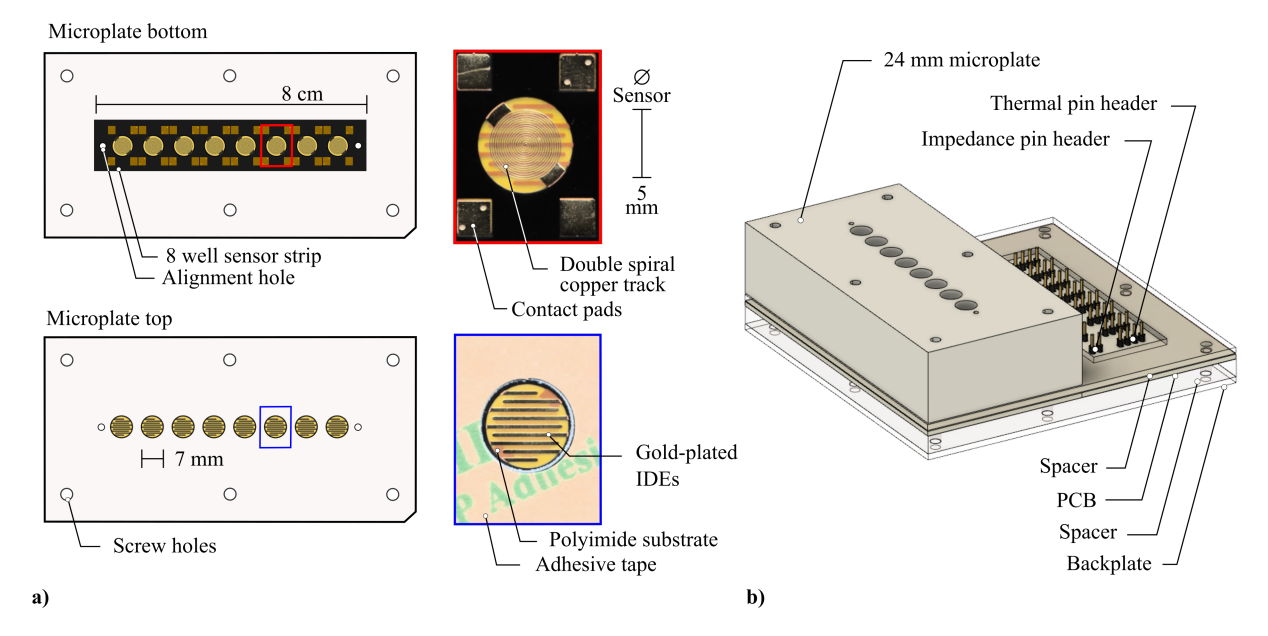


Fig. 2. **Sensor characteristics and schematic overview: a)** Illustrations of the top and bottom side of the microplate with the attached sensor strip containing eight individual impedance and thermal sensing elements. The spiral heating element situates itself on the back side of the sensing strip. The impedance sensing element (IDE) is located on the front side. **b)** Illustration of the microplate measuring setup. The microplate with integrated sensors can be attached to the baseplate (PCB). Read-out hardware can be connected via the thermal and impedance pin header.

0.120 W, cooling time 59 s, sample frequency 100 Hz. Slopes of the transient curves were analysed at  $[0.25\text{-}1] \text{ s}^{1/2}$ ; the first part of the slopes were ignored as this interval indicates the heating pulse propagating through the sensor's substrate.

Impedance spectra were recorded with following measuring settings: bias voltage 0 V, oscillating voltage 0.05 V, minimum frequency 10 kHz, maximum frequency 100 kHz, 5 frequencies per decade. The magnitude of the impedance signal at a frequency of 56 kHz was selected for liquid identification.

#### C. Measuring Protocol

The measuring protocol is based on the measurement of a reference to exclude sensor variation on the raw sensor signal. As this liquid only serves a role as reference and does not influence the measurement, a highly conductive liquid was arbitrarily chosen (4% NaCl in MilliQ). The measurement started out with the loading of the reference liquid into the wells (500 µl). After the wells were filled, the thermal analyser was started to sequentially measure the eight channels one after another. As the thermal measuring technique is based on the generation of heat, caution should be taken when simultaneously measuring impedance [29]. As temperature highly influences the impedance data, a small delay (approximately 30 seconds) between the measuring of the thermal and electrical properties was built-in. Consequently, the thermal and impedance analysers ran in sync, with this small delay, measuring all channels sequentially. After the collection of five thermal and impedance datapoints, the wells were cleaned with pure water and dried out after which the measurable sample was inserted (500 µl). Here again, five datapoints were collected of each sample. The timely procedure is also visualised in the results section (Figure 4). To reference the obtained impedance and slope data, the difference in signal

was calculated between the five individual sample data points and the average reference signal using the following equation:  $[(X_{sample}-X_{reference})/X_{sample}].$ 

#### D. Combined Thermal and Impedance Analysis on Glycerol/Water Dilutions with Various Additions of NaCl

As a proof-of-concept, different glycerol/water dilutions were measured with various additions of NaCl (Glycerol: 99.6% VWR Chemicals, Milli-Q: Atrium pro VF Sartorius, NaCl: 100.0% VWR Chemicals). Because of the difference in thermal properties (Glycerol: 906 Ws<sup>1/2</sup>/m<sup>2</sup>K, Water: 1588 Ws<sup>1/2</sup>/m<sup>2</sup>K [36]), a dilution of both liquids varies the thermal properties as such. Whilest on the other hand, the addition of ions (in the form of NaCl) induces a higher electrical conductivity. Five different glycerol/water dilutions were prepared (0, 12.5, 25, 37.5, and 50%), each for four different NaCl conditions (1, 2, 3, and 4%). Because of the differences in density (glycerol: 1.26 g/cm<sup>3</sup>, Milli-Q: 1 g/cm<sup>3</sup>) [37], [38] and NaCl-solubility (glycerol: 83g NaCl/kg solvent, Milli-Q: 360g NaCl/kg solvent) [39], all dilutions were made based on weight percentages (wt%). Additionally, as a result of the high viscosity of glycerol, a maximum of 50% of glycerol was maintained to ensure the samples could be handled using standard lab pipettes. As a reference liquid, 4% NaCl in pure Milli-Q was used. All 20 different sample variations were measured in 8 wells, using the measuring procedure as described above. Out of these 160 individual measurements, 5 were excluded due to technical or human errors (pipetting mistake, loose wires, etc.).

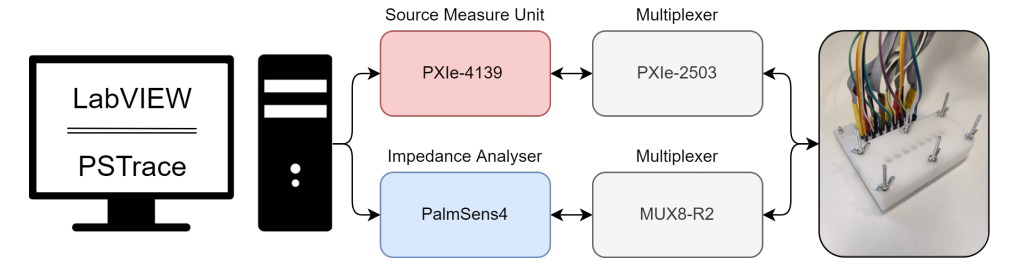


Fig. 3. Schematic overview of the sensor setup with the corresponding hardware and software. Both the thermal and impedance setups are connected to the same desktop computer and analysed simultaneously.

## E. Combined Thermal and Impedance Analysis for Liquid Identification on Fruit Juices

As a proof-of-application, liquid identification was performed on various fruit juices. Seven different fruit juices were examined: apple, grape, grapefruit, mango, orange, pear, and pineapple (Albert Heijn B.V., Zaandam). To exclude the interference of fruit pulp to the sensing element, all juices were filtered (Whattman 113, Sigma-Aldrich) before measuring. As a reference liquid, 4% NaCl in pure Milli-Q was used. All seven different samples were measured in all eight wells, using the measuring procedure as described above. All 56 measurements are included in the processing; no outliers were removed. A Gaussian Mixture Model (Scikit-learn Python) was used to cluster and label the data.

#### IV. RESULTS AND DISCUSSION

#### A. Combined Thermal and Impedance Analysis on Glycerol/Water Dilutions with Various Additions of NaCl

To assess whether the sensor can simultaneously measure thermal and electrical properties, different dilutions of glycerol and water combined with various additions of salt were measured. The reasoning behind this experimental setup is that when changing the dilution of this mixture, mainly the thermal properties of the sample varies. Glycerol has a thermal effusivity of 906 Ws<sup>1/2</sup>/m<sup>2</sup>K and water of 1588 Ws<sup>1/2</sup>/m<sup>2</sup>K [36], a dilution of both liquids varies its thermal effusivity as such. While on the other hand, by introducing more ions to these dilutions by the addition of salt, mainly the electrical property varies.

Figure 4 shows the measuring procedure, specifically of 25% glycerol in water with 2% NaCl, visualizing the (a) magnitude change |Z| at a frequency of 56 kHz and (b) slope change between the reference (4% NaCl in water) and this particular sample. At the start, the reference sample was measured until five thermal and impedance data points were collected. Then, when both read-out methods acquired five distinct datapoints, the reference was cleaned out and the sample was inserted, followed by the collection of again five data points. This way, the thermal and electrical properties are measured parallel in time. The average reference value is used to calculate the relative difference of the raw sample data to the reference sample. The graph clearly shows the high intrasensor stability; a very low deviation on both the thermal and impedance data can be seen in each channel separately ( $SD_Z$ 

= 0.037%,  $SD_{Slope}$  = 0.012%). On the other hand, the intersensor deviation is higher; the different channels can visibly be distinguished ( $SD_Z$  = 3.159%,  $SD_{Slope}$  = 0.176%). Please refer to Table I for the sensor specific mean and standard deviation. As mentioned earlier, the choice of measuring frequency can impact which characteristic of the sample is measured: capacitive of resistive behaviour. Therefore, impedance spectra were recorded for a range of frequencies to construct a Bode plot (Supplementary Material). As this research focusses on the identification of liquids, a higher measuring frequency regime was chosen (56 kHz), indicating the resistive properties of the bulk liquid [33].

Table I shows that the inter-sensor SD is the most contributing factor to read-out precision. Therefore, in all other following experiments, the sensor average is shown as one value, hence to high intra-sensor stability. Additionally, this phenomenon was observed in all subsequent measured sam-

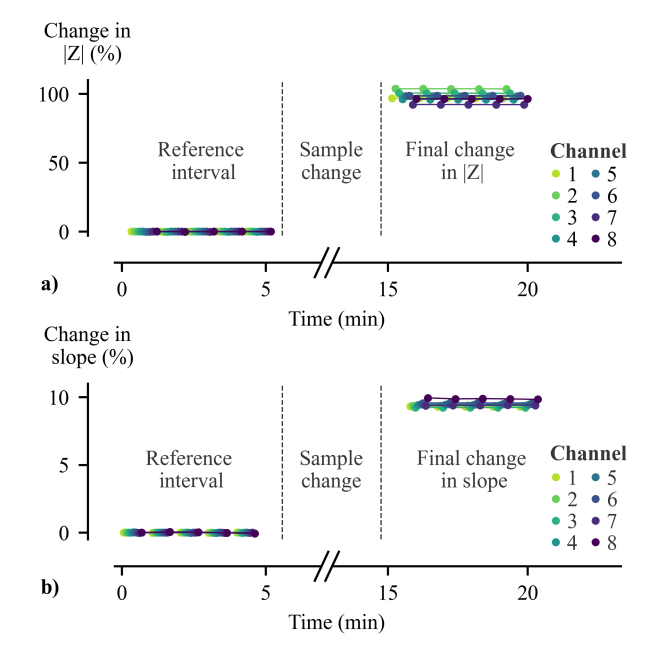


Fig. 4. Measuring procedure: 25% glycerol in water with 2% NaCl: a) The change in magnitude |Z| at a frequency of 56 kHz and b) change in slope during the whole measurement procedure containing data from the reference and sample. The first five datapoints measured 4% NaCl as reference, after which the reference was cleaned out and the sample was inserted. At last, five distinct datapoints from the sample were collected.

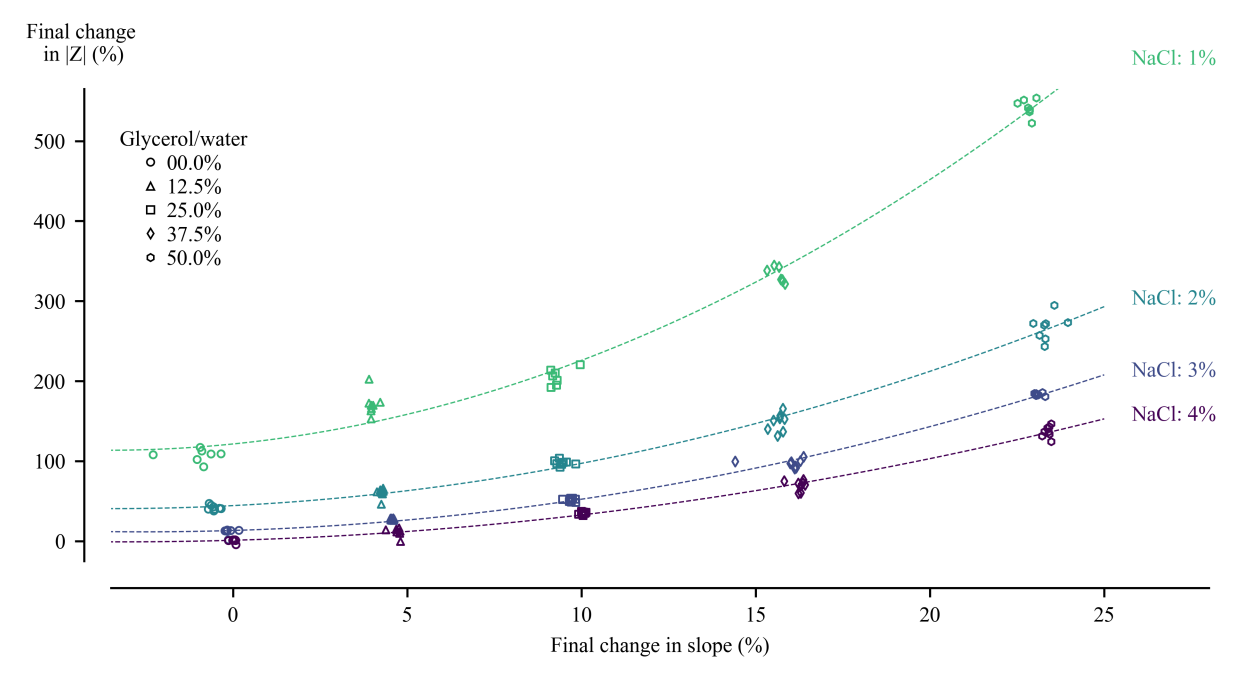


Fig. 5. Combined analysis of thermal and impedance-based measurements on glycerol/water dilutions with various additions of NaCl: Five different glycerol/water dilutions (wt%) were measured in combination with four NaCl conditions. The final change in slope (sensor average) reflects the thermal effusivity of the sample and is plotted on the x-axis. The final change in magnitude (sensor average) reflects the electrical resistance and is plotted on the y-axis. Every sample was measured eight times, each in a different channel, resulting in eight datapoints (sensor average) per condition.

ples.

The measuring protocol was repeated for every glycerol/water dilution with various additions of NaCl. The final magnitude and slope change-values (as visualised in Figure 4) are exported, averaged, and plotted in function of each other per sample condition. This low-level data fusion technique sufficiently allows for liquid identification, see Figure 5. Each datapoint resembles the average data from one sensor, resulting in eight datapoints per sample. 4% NaCl in water was used as reference, hence the resulted measurement is equal to 0% change in both magnitude and slope.

In Figure 5, it shows that the final change in slope is mainly dictated by the ratio of glycerol/water because of their vastly thermal differences. The higher the content of glycerol

TABLE I
MEASUREMENT-DATA CHARACTERISTICS
GLYCEROL 25% NACL 2%

	Impedance		Thermal	
	Mean  Z  change [%]	SD [%]	Mean slope change [%]	SD [%]
Channel 1	96.891	0.021	9.298	0.006
Channel 2	103.632	0.037	9.367	0.012
Channel 3	100.435	0.065	9.226	0.008
Channel 4	95.900	0.063	9.429	0.008
Channel 5	98.276	0.019	9.475	0.009
Channel 6	98.607	0.031	9.569	0.002
Channel 7	92.188	0.032	9.386	0.012
Channel 8	96.366	0.023	9.836	0.037
Inter-sensor SD	3.159	-	0.176	-
Intra-sensor SD	-	0.037	-	0.012

in this mixture, the greater the slope change is recorded, which is in accordance to the thermal effusivity values of these liquids. Besides, the data shows that the salt content can slightly influence the thermal properties of the sample as well. The thermal property differences due to the saline content is limited, yet in concordance with literature [40]. This confirms that not all salt conditions for a particular dilution should confine to the same final slope value, as shown in our recordings.

Additionally, as shown in Figure 5, the presence of more salt induces the conductivity of the sample. When lowering the salt content in the sample, the magnitude of resistance at 56 kHz increases. As pure glycerol and Milli-Q have both an extremely low electrical conductivity, the lowest NaCl condition was set at 1% to ensure a measurable impedance signal. Although both liquids are minimally conductive, our recordings show that the conductivity of the sample seems to be influenceable by the mixing ratio of glycerol/water. Even though this could be a result of a numerous amount of product characteristics, it was experimentally confirmed that the glycerol is less conductive than the Milli-Q used in our experiments (Supplementary Material), explaining the discrepancy.

In conclusion, these measurements show that the sensor is capable to measure a range of samples with various electrical and thermal properties in parallel with a high precision. In theory, this dataset could be further used to analyse glycerol/water/NaCl solution for liquid identification, yet falls beyond the scope of this research as this serves more to demonstrate the combined sensing principle.

## B. Combined Thermal and Impedance Analysis for Liquid Identification on Fruit Juices

As a proof-of-application of the combined analysis, the sensor's measuring capability is studied in the identification of fruit juices. Seven different fruit juices (apple, grape, grapefruit, mango, orange, pear, and pineapple) were analysed according to the basic measuring protocol as used above (measuring all samples in eight wells). Again, 4% NaCl in water was used as the reference sample. The differences in magnitude and slope were recorded and plotted in function of each other. The results are shown in Figure 6. A low-level data fusion technique (Gaussian Mixture Model) determines the data clusters and assigns the colors. A legend was manually added afterwards.

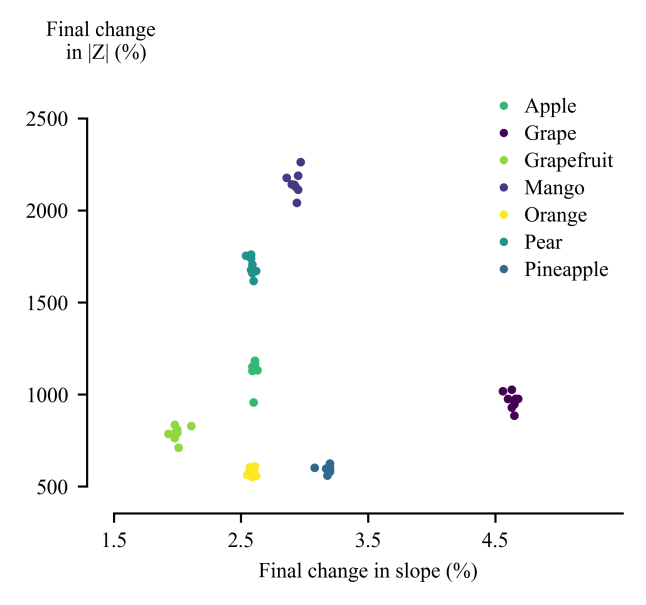


Fig. 6. Cluster analysis to identify fruit juices based on the combined analysis of thermal and impedance data: Seven different fruit juices were measured and analysed based on their electrical and thermal properties. The final change in slope reflects the thermal effusivity of the sample and is plotted on the x-axis. The final change in magnitude reflects the electrical resistance and is plotted on the y-axis. All juices were measured eight times, each in a different channel, resulting in eight datapoint (sensor averages) per condition. A Gaussian Mixture Model was used to cluster and label the data points. A legend was manually added.

The results show that the various fruit juices used in this experiment have a wide variety of electrical and thermal properties, resulting in different recorded final changes in magnitude and slopes. The differences in thermal properties are relatively low, yet adequate to distinguish the different juices. In contrast, the differences in electrical properties are much more pronounced, resulting in much greater differences in the recorded magnitude changes. Table II shows the juice-specific mean change in magnitude |Z| and slopes measured in eight channels. It should be apparent that these liquids, compared to the lab-grade glycerol and Milli-Q in the experiment above, are a lot more complex and could influence the measuring precision. Table II shows that the standard deviation is higher amongst these juices, yet proves to be precise enough to differentiate the juices.

Via a Gaussian Mixture Model, different data clusters could be achieved, indicating the different juices. A Rand-Index of 1 was obtained; all datapoints were assigned to the right fruit juice data cluster. In turn, this plot highlights the most important feature of the combined analysis; the distinctive capacity to identify the liquids increases. Even when used separately, both sensing techniques could distinguish between most tested juices. However, when one would solely analyse the thermal data, the data points from different juices could overlap (f.e. Pear, Orange, and Apple). Likewise, based on solely the EIS data, the datapoints of Orange and Pineapple juice would overlap. However, the Gaussian Mixture Method confirms that all juices could be clustered and distinguished from each other by combining both datasets.

TABLE II
MEASURED FRUIT JUICES CHARACTERISTICS

	Impedance		Therr	Thermal	
	Mean  Z  change [%]	SD [%]	Mean slope change [%]	SD [%]	
Apple	1125.187	67.031	2.603	0.017	
Grape	965.900	43.759	4.634	0.036	
Grapefruit	789.478	37.150	2.003	0.052	
Mango	2148.300	61.950	2.929	0.035	
Orange	578.254	20.571	2.587	0.026	
Pear	1697.130	49.160	2.584	0.025	
Pineapple	592.812	18.615	3.180	0.046	

#### V. CONCLUSION

In the presented work, an innovative combined sensor design to analyse thermal properties and electrical impedance in a high-throughput format is shown. Initially, the capability of the sensor to measure both measurands in parallel was established. This measurement was repeated for a wide array of glycerol/water dilutions with various additions of NaCl. The obtained data was fused together in one plot to create an overview of these sample characteristics. This plot showed that a wide range of thermal and electrical properties can be measured using this combined measuring principle.

To demonstrate the power of the combined analysis, a proof-of-application experiment was executed. Seven different fruit juices were measured using the proposed sensor measuring techniques and a combined analysis was performed. The results highlight the most important feature; the distinctive capacity increases drastically when using two different readout methods to analyse liquids simultaneously. Cluster analysis (Gaussian Mixture Model) clearly shows the distinct juices (Rand-Index = 1).

Since this research merely serves as a demonstrator for this combined read-out technique, the potential application domain is yet undiscovered. Both methods are attractive read-out methods on their own, yet when combined, could excel even further. The combined measuring platform has great potential to develop advanced diagnostics in various fields such as healthcare, biology, or food quality. Since both methods already serve as tools in these sectors, the combination could prove extremely powerful. Especially when time-dependent

processes need to be monitored, the added advantage of measuring two different read-outs simultaneously can be of added value.

#### **ACKNOWLEDGMENT**

The authors would like to thank Makerspace PXL/UHasselt for the technical support.

#### REFERENCES

- R. C. Luo and C.-C. Chang, "Multisensor fusion and integration: A review on approaches and its applications in mechatronics," *IEEE Transactions on Industrial Informatics*, vol. 8, no. 1, pp. 49–60, 2011.
- [2] B. D. Majumder, J. K. Roy, and S. Padhee, "Recent advances in multifunctional sensing technology on a perspective of multi-sensor system: A review," *IEEE Sensors Journal*, vol. 19, no. 4, pp. 1204– 1214, 2018.
- [3] M. A. Najeeb, Z. Ahmad, R. Shakoor, A. Mohamed, and R. Kahraman, "A novel classification of prostate specific antigen (psa) biosensors based on transducing elements," *Talanta*, vol. 168, pp. 52–61, 2017.
- [4] N. A. Mungroo and S. Neethirajan, "Biosensors for the detection of antibiotics in poultry industry—a review," *Biosensors*, vol. 4, no. 4, pp. 472–493, 2014.
- [5] M. Gustavsson, H. Nagai, and T. Okutani, "Thermal effusivity measurements of insulating liquids using microsized hot strip probes," *Review of Scientific Instruments*, vol. 74, no. 10, pp. 4542–4548, 2003.
- [6] C. Grosse, M. A. Ras, A. Varpula, K. Grigoras, D. May, B. Wunderle, P.-O. Chapuis, S. Gomès, and M. Prunnila, "Microfabricated sensor platform with through-glass vias for bidirectional 3-omega thermal characterization of solid and liquid samples," *Sensors and Actuators A: Physical*, vol. 278, pp. 33–42, 2018.
- [7] S. E. Gustafsson, E. Karawacki, and M. N. Khan, "Transient hot-strip method for simultaneously measuring thermal conductivity and thermal diffusivity of solids and fluids," *Journal of Physics D: Applied Physics*, vol. 12, no. 9, p. 1411, 1979.
- [8] "Plastics Determination of Thermal Conductivity and Thermal Diffusivity Part 2: Transient Plane Heat Source (Hot Disc) Method," International Organization for Standardization, Standard, Aug. 2015.
- [9] G. Oudebrouckx, J. Goossens, S. Bormans, T. Vandenryt, P. Wagner, and R. Thoelen, "Integrating thermal sensors in a microplate format: Simultaneous real-time quantification of cell number and metabolic activity," ACS Applied Materials & Interfaces, 2022.
- [10] S. E. Gustafsson, "Transient plane source techniques for thermal conductivity and thermal diffusivity measurements of solid materials," *Review of Scientific Instruments*, vol. 62, no. 3, pp. 797–804, 1991.
- [11] S. A. Al-Ajlan, "Measurements of thermal properties of insulation materials by using transient plane source technique," *Applied Thermal Engineering*, vol. 26, no. 17-18, pp. 2184–2191, 2006.
- [12] Q. Ai, Z.-W. Hu, L.-L. Wu, F.-X. Sun, and M. Xie, "A single-sided method based on transient plane source technique for thermal conductivity measurement of liquids," *International Journal of Heat and Mass Transfer*, vol. 109, pp. 1181–1190, 2017.
- [13] A. Harris, S. Kazachenko, R. Bateman, J. Nickerson, and M. Emanuel, "Measuring the thermal conductivity of heat transfer fluids via the modified transient plane source (mtps)," *Journal of Thermal Analysis* and Calorimetry, vol. 116, no. 3, pp. 1309–1314, 2014.
- [14] G. Oudebrouckx, T. Vandenryt, P. Nivelle, S. Bormans, P. Wagner, and R. Thoelen, "Introducing a thermal-based method for measuring dynamic thin film thickness in real time as a tool for sensing applications," *IEEE Transactions on Instrumentation and Measurement*, vol. 70, pp. 1–10, 2020.
- [15] S. E. Gustafsson, M. A. Chohan, K. Ahmed, and A. Maqsood, "Thermal properties of thin insulating layers using pulse transient hot strip measurements," *Journal of Applied Physics*, vol. 55, no. 9, pp. 3348– 3353, 1984.
- [16] G. Oudebrouckx, D. Nieder, T. Vandenryt, S. Bormans, H. Möbius, and R. Thoelen, "Single element thermal sensor for measuring thermal conductivity and flow rate inside a microchannel," *Sensors and Actuators A: Physical*, vol. 331, p. 112906, 2021.
- [17] S. Bormans, G. Oudebrouckx, P. Vandormael, T. Vandenryt, P. Wagner, V. Somers, and R. Thoelen, "Pulsed thermal method for monitoring cell proliferation in real-time," *Sensors*, vol. 21, no. 7, p. 2440, 2021.

- [18] M. Grossi and B. Riccò, "Electrical impedance spectroscopy (eis) for biological analysis and food characterization: A review," *Journal of Sensors and Sensor Systems*, vol. 6, no. 2, pp. 303–325, 2017.
- [19] X. Liu, J. Xiong, Y. Lv, and Y. Zuo, "Study on corrosion electrochemical behavior of several different coating systems by eis," *Progress in Organic Coatings*, vol. 64, no. 4, pp. 497–503, 2009.
- [20] N. Tang, W. J. van Ooij, and G. Górecki, "Comparative eis study of pretreatment performance in coated metals," *Progress in Organic Coatings*, vol. 30, no. 4, pp. 255–263, 1997.
- [21] S. Kabir, D. Ghosh, and N. Islam, "Applications of electrochemical impedance spectroscopy (eis) for various electrode pattern in a microfluidic channel with different electrolyte solutions," in ASME International Mechanical Engineering Congress and Exposition, vol. 85666. American Society of Mechanical Engineers, 2021, p. V010T10A042.
- [22] E. P. Randviir and C. E. Banks, "Electrochemical impedance spectroscopy: an overview of bioanalytical applications," *Analytical Methods*, vol. 5, no. 5, pp. 1098–1115, 2013.
- [23] S. Siddiqui, Z. Dai, C. J. Stavis, H. Zeng, N. Moldovan, R. J. Hamers, J. A. Carlisle, and P. U. Arumugam, "A quantitative study of detection mechanism of a label-free impedance biosensor using ultrananocrystalline diamond microelectrode array," *Biosensors and Bioelectronics*, vol. 35, no. 1, pp. 284–290, 2012.
- [24] A. P. Guttenplan, S. Bormans, Z. Tahmasebi Birgani, M. Schumacher, S. Giselbrecht, R. K. Truckenmüller, P. Habibović, and R. Thoelen, "Measurement of biomimetic deposition of calcium phosphate in real time using complex capacitance," *Physica Status Solidi* (a), p. 2000672, 2021.
- [25] M. Lemmens, H. Biesmans, S. Bormans, T. Vandenryt, and R. Thoelen, "Electrical impedance tomography with a lab-on-chip for imaging cells in culture," *physica status solidi (a)*, vol. 215, no. 15, p. 1700868, 2018.
- [26] H.-R. Tränkler, O. Kanoun, M. Min, and M. Rist, "Smart sensor systems using impedance spectroscopy," *Proc. Estonian Acad. Sci. Eng*, vol. 13, no. 4, pp. 455–478, 2007.
- [27] G. Luciani, R. Ramilli, A. Romani, M. Tartagni, P. Traverso, and M. Crescentini, "A miniaturized low-power vector impedance analyser for accurate multi-parameter measurement," *Measurement*, vol. 144, pp. 388–401, 2019.
- [28] M. Jaegle, H.-F. Pernau, M. Pfützner, M. Benkendorf, X. Li, M. Bartel, O. Herm, S. Drost, D. Rutsch, A. Jacquot et al., "Thermal-electrical impedance spectroscopy for fluid characterisation," *Procedia Engineer*ing, vol. 168, pp. 770–773, 2016.
- [29] R. Sauerheber and B. Heinz, "Temperature effects on conductivity of seawater and physiologic saline, mechanism and significance," *Chem. Sci. J*, vol. 6, p. 109, 2015.
- [30] D. Reyes-Romero, O. Behrmann, G. Dame, and G. Urban, "Dynamic thermal sensor for biofilm monitoring," *Sensors and Actuators A: Physical*, vol. 213, pp. 43–51, 2014.
- [31] R. Firstenberg-Eden and J. Zindulis, "Electrochemical changes in media due to microbial," *Journal of Microbiological Methods*, vol. 2, no. 2, pp. 103–115, 1984.
- [32] A. Sizov, D. Cederkrantz, L. Salmi, A. Rosén, L. Jacobson, S. Gustafsson, and M. Gustavsson, "Thermal conductivity versus depth profiling of inhomogeneous materials using the hot disc technique," *Review of Scientific Instruments*, vol. 87, no. 7, p. 074901, 2016.
- [33] S. M. M. Alavi, A. Mahdi, S. J. Payne, and D. A. Howey, "Identifiability of generalized randles circuit models," *IEEE Transactions on Control Systems Technology*, vol. 25, no. 6, pp. 2112–2120, 2016.
- [34] "ANSI/SLAS Microplate Standards." [Online]. Available: https://www.slas.org/education/ansi-slas-microplate-standards/
- [35] "96-Well Plate Dimensions BRANDplates Standard 96-Well Microplates." [Online]. Available: https://www.wellplate.com/96-wellplate-dimensions/
- [36] "Materials Database Thermal Properties Thermtest Inc." [Online]. Available: https://thermtest.com/thermal-resources/materials-database
- [37] "Glycerine (glycerol) Ph. Eur., USP, BP VWR." [Online]. Available: https://nl.vwr.com/store/product/734996/glycerine-glycerol-ph-eur-usp-bp
- [38] "Liquids Densities." [Online]. Available: https://www.engineeringtoolbox.com/liquids-densities-d743.html
- [39] J. Burgess, Metal Ions in Solution. Ellis Horwood, 1978.
- [40] "Thermal Conductivity of Salty Water Mixtures (Water + NaCl)." [Online]. Available: https://thermtest.com/application/thermal-conductivity-of-salty-water-mixtures



**Juul Goossens** received the M.Sc. degree in biomedical sciences with a specialisation in bioelectronics and nanotechnology from Hasselt University, Hasselt, Belgium, in 2021, where he is currently pursuing the Ph.D. degree.

He joined the Biomedical Device Engineering Group, Institute for Materials Reseach (IMO-IMOMEC), Hasselt University. His current research focusses on the development of sensing technology aimed at the food industry. Most recently, his work involved the integration of ther-

mal and impedance sensors into a microplate format, which shows great promise for biological applications.



Souhaib El Habti received the M.Sc. degree in electronic/ICT (information and communication Technology) engineering from Hasselt University, Hasselt, Belgium, in 2022.

He is currently working as an Account Engineer at Neways in Echt, Netherlands.



Seppe Bormans received the M.Sc. degree in electronic/information and communications technology (ICT) engineering with a specialisation in e-Health from Hasselt University, Hasselt, Belgium, in 2016, where he is currently pursuing the Ph.D. degree.

He then joined the Biomedical Device Engineering Group, Institute for Materials Reseach (IMO-IMOMEC), Hasselt University. His current research focuses on the development of thermal and impedance sensor technology for biomedi-

cal/biological applications of which thermally monitoring cell growth in a real-time manner is the most innovative.



Mohammad Mahdavinasab received the M.Sc. in mechanical engineering with a major in energy transformation from Semnan University, Semnan, Iran in 2020. He is currently pursuing the Ph.D. degree with the Biomedical Device Engineering Group, institute for material research (IMO-IMOMEC), Hasselt University.

His current research focuses on development of thermal and impedance sensor technology for monitoring microfluidics. Most recently, his work involves integrating thermal sensors into a

microfluidic mixing device.



Gilles Oudebrouckx received his MSc in electronic engineering (2016), with a major in embedded systems, from Hasselt University. In 2021 he obtained his Ph.D. in engineering technology at the Institute for Materials Research (IMO-IMOMEC) of Hasselt University. His doctoral research involved the development of thermal sensors and thermal sensing principles aimed at biological applications.

Currently, he is a Postdoctoral Fellow at IMO-IMOMEC. His current work focuses on transfer-

ring novel thermal sensor technology to industry.



Ronald Thoelen received the master's degree in applied physics from the Eindhoven University of Technology (TU Eindhoven), Eindhoven, The Netherlands, in 2004, and the Ph.D. degree in physics with a focus on impedance-based biosensors from Hasselt University (UHasselt), Hasselt, Belgium, in 2008.

He is currently a Full Professor within the Faculty of Engineering Technology, Hasselt University, where he is also the Leader of the research group Biomedical Device Engineering

within IMO-IMOMEC; the group develops advanced diagnostic systems for screening the presence of various molecules in aqueous solutions. He is also the Head of education of the Electronics & Information and Communications Technology (ICT) Master Program of his Faculty of Engineering Technology. His research focuses on the development of "dedicated" sensor devices in environmental, food, and health(care) domains



Thijs Vandenryt received the bachelor's degree in electronics, after an internship, form the Universidade de Vigo, Vigo, Spain, in 2006, and the M.Sc. degree in electrical engineering from XIOS Hogeschool Limburg, Limburg, Belgium, in 2008. He is currently pursuing the Ph.D. degree with Hasselt University, Hasselt, Belgium, with a strong focus on microfluidics and biomedical system integration.

He is currently with the Biomedical Device Engineering Group, Hasselt University, where he

is involved in several international projects, designing, and building electronics and microfluidics for sensing applications.